Weak-value amplification of light deflection by a dark atomic ensemble

Lan Zhou (周兰),[1] Yusuf Turek (玉素甫•吐拉克),[2] C. P. Sun (孙昌璞),[3] and Franco Nori (野理)[4,5]

[1] *Key Laboratory of Low-Dimensional Quantum Structures and Quantum Control of Ministry of Education, and Department of Physics, Hunan Normal University, Changsha 410081, China*

[2] *State Key Laboratory of Theoretical Physics, Institute of Theoretical Physics, University of Chinese Academy of Science, Beijing 100190, China*

[3] *Beijing Computational Science Research Center, Beijing 100084, China*

[4] *CEMS, RIKEN, Saitama, 351-0198, Japan*

[5] *Physics Department, The University of Michigan, Ann Arbor, Michigan 48109-1040, USA*

(Received 17 February 2013; published 13 November 2013)

We study the coherent propagation of light whose dynamics is governed by the effective Schrödinger equation derived in a magneto-optically manipulated atomic ensemble with a four-level tripod configuration for electromagnetically induced transparency (EIT). The small transverse deflection of an optical beam, which is ultrasensitive to the EIT effect, could be drastically amplified via a weak measurement with an appropriate preselection and postselection of the polarization state. The physical mechanism is explained as the effect of wave-packet reshaping, which results in an enlarged group velocity in the transverse direction.

DOI: 10.1103/PhysRevA.88.053815 PACS number(s): 42.50.Gy, 03.65.Ta, 42.25.Ja

I. INTRODUCTION

The weak measurement proposed by Aharonov, Albert, and Vaidman [1,2] is usually referred to as an amplification effect for weak signals rather than a conventional quantum measurement that collapses a coherent superposition of quantum states [3]. In the original gedanken experiment [1], a seemingly surprising effect was proposed: that it is possible to "measure" an appropriate preselected state of a spin-$1/2$ particle to obtain the average spin beyond the bound $[-0.5,0.5]$ of the smallest and largest eigenvalues. Such an average spin (called a weak value) does not exactly reflect the reality of a single spin, and is only the ensemble average of the measured data over a postselected subset. In this sense, the weak measurement implies some amplification of the resulting signal in the apparatus carrying on the pre- and postselections [4]. Several groups have studied this weak-value amplification (WVA) effect in various physical systems, such as quantum-optical [5–8] and condensed-matter systems [9,10]. Note that WVA has been utilized as a quantum-coherent manipulation to engineer various interesting quantum effects, such as superluminal effects in birefringent optical fibers [11], ultrasensitive beam deflection [7], and optical spin-Hall effects [12–16].

In this paper, we study the weak-value problem of spin $1/2$ with polarized light beams propagating in a dispersive medium, a four-level atomic ensemble controlled by external fields. The motion of the light-wave envelope in such a coherent medium is described by an effective Schrödinger equation resembling the precession of a spin $1/2$ in an inhomogeneous magnetic field [17–20]. However, because the effective magnetic field is very weak due to the inhomogeneity of the coupling transitions, the deflection of the light beam is usually difficult to observe even for electromagnetically induced transparency (EIT) with two-photon resonance. For example, in the experiment by Karpa and Weitz [21], the angle of deflection is only about 2×10^{-5} rad when the light passes through a gas cell 5 cm long.

Since our concern here is only the deflection of the optical beam rather than the enhancement of the beam split, and the two split beams may be deflected in the same direction, we consider weak measurements to achieve this goal. We note that protocols based on weak measurements are probabilistic. In reality, our goal is achieved by throwing away most of the data in the postselection process. However, it does not impede the further application of postselections. A few postselections are still appropriate to demonstrate basic physics features and quantum-information processes; for example, postselection has been used to: obtain the correct logical output [22] and to generate entanglement. This kind of postselected entanglement was used to violate Bell's inequality [23]. According to our previous series of studies [17–20], the motion of the transverse wave packet is described by a Schrödinger-like equation, similar to that for a spin $1/2$ in a transversely inhomogeneous magnetic field in a Stern-Gerlach experiment [20]. Thus, the peak of the optical beam will split into two, according to the initial polarization, under the influence of the transverse magnetic field gradient. When making a postselection on the final polarized state, the projection on this chosen polarization state mixes the two local wave packets in the transverse split. If such a weak measurement does not deform the shape of the wave packet too much, the transverse distance of the reshaped wave packet from the center of the beam may be very large compared to that for any peaks in an optical Stern-Gerlach experiment. We carry out the relevant calculations in detail by making use of the effective field approach [24,25].

This paper is organized as follows. In Sec. II, we present a theoretical model for a four-level atomic ensemble with a tripod configuration in the presence of nonuniform external fields and derive the system of equations for the dynamics of the signal field in the atomic linear response with respect to the probe field. In Sec. III, we present the optical Stern-Gerlach effect of the probe beam in momentum space, which is induced by the interaction between the dispersive atomic medium and the probe field used for EIT. In Sec. IV, we theoretically study the transverse deflection of the probe field via weak measurements, which can amplify signals by appropriate

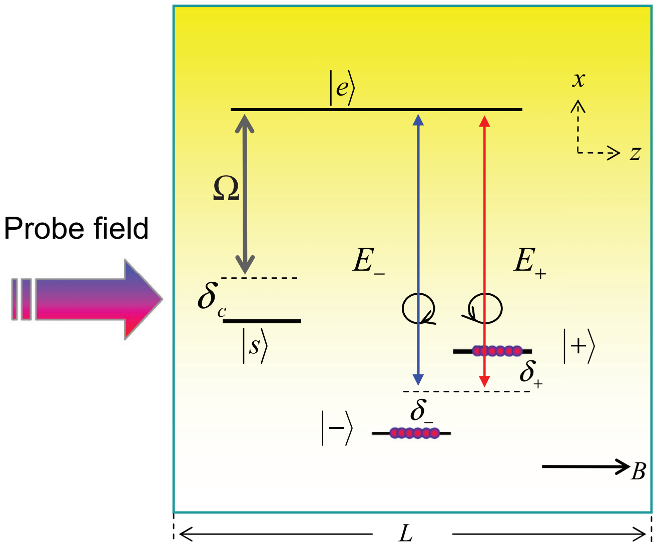

FIG. 1. (Color online) Schematic diagram of an atomic ensemble with a four-level tripod configuration in a gas cell of length L, manipulated by two optical and one magnetic field. The magnetic field B is applied along the z direction with a gradient along the x direction.

preselected and postselected states of the system. We conclude our paper in the final section.

II. MODEL SETUP

Consider an ensemble of N identical and noninteracting atoms confined in a rectangular gas cell, characterized by the ground-state Zeeman sublevels $|\pm\rangle$, one intermediate state $|s\rangle$, and an excited state $|e\rangle$, as shown in Fig. 1. The levels are coupled by two optical fields: a control laser field with frequency ν_c and wave number k_c, and a probe laser field with frequency ν and wave number k. The control field is assumed to be homogeneous and strong enough for propagation effects to be neglected, and it was tuned to the $|s\rangle \rightarrow |e\rangle$ transition. The coupling strength is characterized by the Rabi frequency Ω. Here, the Rabi frequency Ω is taken to be a constant throughout the paper. The probe laser field is linearly polarized and propagating along the z axis. Its linear polarization is a superposition of left- and right-handed circular polarization, labeled by $\sigma_\pm$. We denote the σ_j-polarized component as $\tilde{E}_j(\mathbf{r},t)$, $j=\pm$, which drive the transitions $|\pm\rangle \leftrightarrow |e\rangle$, respectively.

The atomic gas cell can be divided into many smaller cells. We assume that each smaller cell contains a large number of atoms and the inhomogeneous external field is sufficiently homogeneous for each smaller cell [17]. In this case, the atomic medium can be treated in a continuous way by the following approach. First, describe the medium excitation by introducing the collective atomic operators $\tilde{\Xi}_{\mu\nu}(\mathbf{r}) = (1/N_\mathbf{r})\sum_{j=1}^{N_\mathbf{r}} \tilde{\Xi}_{\mu\nu}^j$, averaged over a small but macroscopic volume containing many atoms $N_\mathbf{r} = (N/V)dV \gg 1$ around position $\mathbf{r}$. Here, $\tilde{\Xi}_{\mu\nu}^j(\mathbf{r}) = |\mu\rangle_j\langle\nu|$. Afterwards replace the sum over the total number N of atoms by $\frac{N}{V}\int d^3r$, where V is the volume of the medium [24,25]. Neglecting the kinetic energy of the atoms, the Hamiltonian of the atomic part is given by

$$H^{(A)} = \frac{N}{V}\sum_i \int d^3r(\omega_i + \mu_i B)\tilde{\Xi}_{ii}, \tag{1}$$

where ω_i $(i=\pm,s,e)$ are the bare atomic energies, and $\omega_\pm = \omega_0$ (which corresponds to degenerate levels when $B=0$). The magnetic field B along the z axis shifts the energy levels by the amount $\mu_i B(\mathbf{r})$, where the magnetic moments $\mu_i = m_F^i g_F^i \mu_B$ are defined by the Bohr magneton μ_B, the gyromagnetic factor g_F^i, and the magnetic quantum number m_F^i of the corresponding state $|i\rangle$. Under the electric-dipole approximation and the rotating-wave approximation, the light-matter interaction Hamiltonian becomes [24,25]

$$\begin{aligned} H^{(I)} = {} & \frac{N}{V}\int \Omega e^{i(\mathbf{k}_c\cdot\mathbf{r}-\nu_c t)}\tilde{\Xi}_{es}d^3r + \text{H.c.} \\ & - \frac{N}{V}\sum_{j=\pm} d_{ej}\int \tilde{E}_j^{(+)}\tilde{\Xi}_{ej}d^3r + \text{H.c.}, \end{aligned} \tag{2}$$

with d_{e-} (d_{e+}) denoting the matrix element of the dipole momentum operator projected on the direction of the electric field.

The slowly varying variables $E_j(\mathbf{r},t)$ for the probe field and the collective atomic transition operators $\Theta_{\alpha\beta}$ can be defined as

$$\tilde{E}_j^+(\mathbf{r},t) = \sqrt{\frac{\nu}{2\varepsilon_0 V}}E_j(\mathbf{r},t)e^{i(kz-\nu t)} \quad (j=\pm), \tag{3a}$$

$$\tilde{\Xi}_{ej} = \Theta_{ej}\exp(-ikz), \tag{3b}$$

$$\tilde{\Xi}_{es} = \Theta_{es}\exp(-i\mathbf{k}_c\cdot\mathbf{r}). \tag{3c}$$

In a rotating reference frame, the dynamics of this system is described by

$$\begin{aligned} H_{\text{rot}} = {} & \frac{N}{V}\int d^3r(\delta_-\Theta_{--} + \delta_+\Theta_{++} + \delta_c\Theta_{ss}) \\ & - \frac{N}{V}\int d^3r\left(\Omega\Theta_{es} + \sum_{j=\pm} g_j E_j\Theta_{ej}\right) + \text{H.c.} \end{aligned} \tag{4}$$

with δ_i $(i=\pm,c)$ the detunings of the probe and control fields from the corresponding atomic transitions given as

$$\delta_c = \omega_s - \omega_e + \nu_c + (\mu_s - \mu_e)B,$$
$$\delta_\pm = \omega_0 - \omega_e + \nu + (\mu_\pm - \mu_e)B,$$

and the coupling strength as

$$g_j = d_{ej}\sqrt{\frac{\nu}{2\varepsilon_0 V}}. \tag{5}$$

The Hamiltonian in Eq. (4) generates the Heisenberg equations of the slowly varying variables $\Theta_{\mu\nu}$. Langevin equations are obtained to describe the dynamics of the medium by introducing the coherence relaxation rate γ between the ground state $|\pm\rangle$ and the intermediate state $|s\rangle$, as well as the decay rate Γ of the excited state. The low-intensity approximation [24–26], on one hand, allows us to neglect Langevin noise operators since the number of photons contained in the probe laser beams is much smaller than the number of atoms in the sample, so the operators become c numbers. On the other hand, it allows us to regard the interaction between the matter and the probe field as a weak disturbance, since the intensity of the probe laser beams is much weaker than that of the control laser field. The perturbation approach [24,25,27] can be applied in terms of a power series in gE_j:

$$\Theta_{\alpha\beta} = \Theta_{\alpha\beta}^{(0)} + \varepsilon\Theta_{\alpha\beta}^{(1)} + \cdots, \tag{6}$$

where ε is a parameter that ranges continuously between zero and 1. When $\varepsilon = 0$, the probe field is absent. For all atoms initially in level $|\pm\rangle$ without polarization (i.e., atom i in a mixed state $\rho_i = \Sigma_{j=\pm}|j\rangle\langle j|/2$), we obtain

$$\Theta_{--}^{(0)} = \Theta_{++}^{(0)} = \tfrac{1}{2} \tag{7}$$

while all others terms vanish. Here, we retain only terms up to the first order in ε, since the linear-optical-response theory can sufficiently reflect the main physical features. The dispersion and absorption are determined by $\Theta_{je}^{(1)}$, which is obtained as

$$\Theta_{je}^{[1]} = \frac{\Delta_j\, g_j\, E_j}{2\Omega\,\Omega^*} \quad (j = \pm) \tag{8}$$

in steady-state solutions [19,20,27], where pure dephasing processes and decay among the lower states are neglected ($\gamma = 0$) to highlight the main physics, and a sufficiently strong driving field is assumed to satisfy $|\Omega|^2 \gg \Gamma\gamma,\delta_i\delta_j$. We note the assumption of the strong driving field implies that $|\Omega| \gg |(\mu_+ - \mu_-)B|$. The Raman detuning is defined as

$$\Delta_j = \delta_j - \delta_c, \tag{9}$$

which leads to a spatially varying refractive index profile in the gas cell [17] due to the small transverse magnetic field gradient.

Using the slowly-varying-envelope approximation, the paraxial wave equation in the linear-optical-response theory [24,25,27]

$$(i\partial_t + ic\partial_z)E_j = -Ng_j^*\Theta_{je}^{(1)}, \tag{10}$$

becomes an effective Schrödinger equation

$$i\partial_t E_j = H_j E_j, \tag{11}$$

by substituting Eq. (8) into (10), where the effective Hamiltonian is

$$H_j = cp_z - \frac{N|g_j|^2}{2|\Omega|^2}\Delta_j. \tag{12}$$

Here c is the velocity of light in vacuum and $p_z = -i\partial_z$. Notice that $\sigma_\pm$ polarizations accompany the component $E_\pm$. Writing the $\sigma_\pm$-polarization states as column vectors resembling the spin 1/2,

$$|\sigma_+\rangle = [\,1\ 0\,]^T, \tag{13a}$$

$$|\sigma_-\rangle = [\,0\ 1\,]^T, \tag{13b}$$

where the superscript T means transpose, we can group the two components $E_\pm$ into a column vector defined as the "spinor state" $\Phi = [E_+,E_-]^T$. The dynamical equation of the probe laser field reads

$$i\partial_t\Phi = \begin{bmatrix} H_+ & 0 \\ 0 & H_- \end{bmatrix}\Phi = H_{\text{eff}}\Phi, \tag{14}$$

which allows us to write the state of the probe laser field at any arbitrary time as

$$|\Phi(t)\rangle = \sum_{j=\pm} c_j|E_j(t)\rangle|\sigma_j\rangle. \tag{15}$$

Here, the states $|E_j\rangle$ describe the state of the spatial degrees of freedom, with $E_j(\mathbf{r},t)$ referred to as the corresponding spatial representation.

Hereafter, to investigate the beam deflection amplification of the light beam, propagating in the dispersive atomic ensemble, we use a signal enhancement technique known from weak measurements [28]. Along with the standard weak-measurement terminology, the transverse-position degree of freedom of the probe beam is referred to as the meter and its intrinsic polarization degree of freedom is referred to as the measured system.

III. OPTICAL STERN-GERLACH EFFECT

We now investigate the evolution of the probe wave packet. The polarization vector of the probe field lies in the plane perpendicular to its traveling direction (i.e., the z direction). It is initially prepared in a superposition state

$$|i\rangle = \cos\frac{\alpha}{2}|H\rangle + \sin\frac{\alpha}{2}|V\rangle \tag{16}$$

of the horizontal polarization, $|H\rangle = (|\sigma_+\rangle + |\sigma_-\rangle)/\sqrt{2}$, and vertical polarization, $|V\rangle = -i(|\sigma_+\rangle - |\sigma_-\rangle)/\sqrt{2}$, where α is the polarization angle of the probe light beam. For weak measurements, this angle is very small, which means that the probe field is initially almost in the horizontal polarization state. The role of α in the transverse beam deflection amplification via weak measurements will be further discussed in the next section.

The two components of the probe field travel collinearly before reaching the medium, which implies that initially $|E_j(t_0)\rangle = |E_0(0)\rangle$, where the initial time $t_0 = 0$. After the probe field enters the medium, the atomic ensemble induces the time evolution operator $U(t) = e^{-iH_{\text{eff}}t}$ on the meter state according to its polarized state. Then the state at an arbitrary time becomes an entangled state

$$|\Phi(t)\rangle = \frac{1}{\sqrt{2}}[e^{-i\alpha/2}|\sigma_+\rangle|E_+(t)\rangle + e^{i\alpha/2}|\sigma_-\rangle|E_-(t)\rangle], \tag{17}$$

where the meter state is described by

$$|E_j(t)\rangle = e^{-iH_jt}|E_0(0)\rangle. \tag{18}$$

We will show that $E_\pm(\mathbf{r},t)$ in Eq. (17) implies a wave-packet split in momentum space according to polarizations. After a measurement on the postselected state $|V\rangle$, the meter is reshaped as

$$\left|\Phi_f^m(t)\right\rangle = \frac{i}{2}[e^{-i\alpha/2}|E_+(t)\rangle - e^{i\alpha/2}|E_-(t)\rangle]. \tag{19}$$

Obviously, the superposition of the two wave packets $E_\pm(\mathbf{r},t)$ can produce an interference pattern in the coordinate space.

Now we assume that the magnetic field B applied in the z direction has a linear gradient along the x direction with the expression

$$B = B_0 + B_1x. \tag{20}$$

Here, our treatment is confined to only one transverse dimension, say the x direction. The effective Hamiltonian in Eq. (12) reads

$$H_j = cp_z + b_{0j} + b_{1j}x, \tag{21}$$

where the parameters

$$b_{0j} = -\frac{N|g_j|^2}{2|\Omega|^2}[\omega_0 + \nu - \omega_s - \nu_c + (\mu_j - \mu_s)B_0], \tag{22a}$$

$$b_{1j} = -\frac{N|g_j|^2}{2|\Omega|^2}(\mu_j - \mu_s)B_1, \tag{22b}$$

can be adjusted by the control laser field and the magnetic field as well as the energy levels. We note that the condition $|\Omega|^2 \gg \Gamma\gamma, \delta_i\delta_j$ guarantees that b_{1j} cannot tend to infinity. For an initial state with a two-dimensional Gaussian amplitude profile

$$E_j(r,0) = \frac{1}{\sqrt{2\pi a^2}}\exp\left(-\frac{z^2+x^2}{4a^2}\right), \tag{23}$$

the EIT medium introduces different phase shifts on the meter wave packet according to whether the state is right-handed or left-handed circularly polarized, and a displacement ct along the z direction,

$$E_j(r,t) = \frac{e^{-itb_{0j}}}{\sqrt{2\pi a^2}}\exp\left[-\frac{(z-ct)^2+x^2}{4a^2} - itb_{1j}x\right]. \tag{24}$$

Since $[H_j,x]=0$, the center of $E_j(\mathbf{r},t)$ does not change with time, $\langle x_j\rangle = 0$, which implies no spatial split of the meter wave packet. A Fourier transformation on Eq. (24),

$$E_j(k,t) = 2\sqrt{2a^2\pi}\exp\left(-ib_{0j}t - a^2k_z^2 - ick_zt\right) \times \exp\left[-a^2\left(k_x + b_{1j}t\right)^2\right], \tag{25}$$

shows that each meter's wave packet keeps the longitudinal momentum unchanged and acquires a transverse momentum with magnitude $b_{1j}t$, which is a linear function of time. Therefore, two wave packets of the probe field have the same centroid, but achieve different momenta in the x direction inside the EIT medium. To illustrate the split of the probe beam in momentum space, we assume that the probe beam with an initial width $a = 2$ mm is tuned to the rubidium (^{87}Rb) D_1 line $5\,^2S_{1/2} \leftrightarrow 5\,^2P_{1/2}$, that the ground states $|\pm\rangle$ correspond to the magnetic sublevels (with $m_F = 1$ and -1) of the $F=1$ hyperfine ground state, and that $|s\rangle$ represents the hyperfine ground state $|F=2, m_F=1\rangle$. In this case, the phase shift on the σ_- component vanishes due to $\mu_s = \mu_- = 4.64\times10^{-24}$ J T^{-1}. Hence, there is no shift of the momentum on the σ_- component. The magnetic field gradient $B_1 = 910\ \mu$G mm^{-1} and the magnetic moments $\mu_+ = -\mu_s$ subject the wave packet of the σ_+ component to a linear potential in the transverse direction. In Fig. 2, we show such an optical Stern-Gerlach effect in momentum space by plotting the transverse distribution $|E_j(k_x,t_f)|^2$ as a function of the wave number $k_x = p_x/\hbar$ using the value $g^2N/\Omega^2 \equiv \tan^2\theta$ given in [29] at a fixed time t_f. (Actually, $g^2N/\Omega^2 \equiv \tan^2\theta$ is obtained from the typical group velocity $v_g = c\cos^2\theta$ of a few thousand meters per second given in Ref. [29].) Here $t_f = L/c$ denotes the interaction time with $L = 50$ mm as the cell length. Obviously, the transverse displacement is smaller than the uncertainty of the width of two wave packets of the meter.

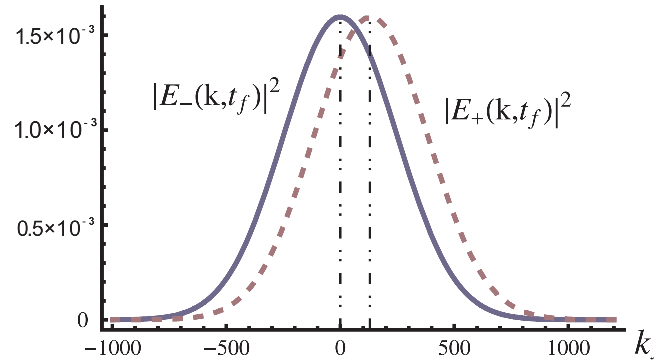

FIG. 2. (Color online) Optical Stern-Gerlach effect in momentum space with the transverse distribution $|E_j(k_x,t_f)|^2$ as a function of wave number $k_x = p_x/\hbar$, right after the light leaves the EIT medium. Here, k_x is in units of reciprocal meters.

However, postselecting the system on a desired polarized state $|V\rangle$ leads to a coherent superposition of two transverse wave packets. The interference of the two meters' wave packets displace the centroid of the wave packet in coordinate space by

$$\langle x\rangle = \frac{\sin(b_0t+\alpha)a^2b_1tf_t}{1 - f_t\cos(b_0t+\alpha)}, \tag{26}$$

where we have introduced $b_0 = b_{0-} - b_{0+}$, $b_1 = b_{1-} - b_{1+}$, and $f_t \equiv \exp(-a^2b_1^2t^2/2)$. We also note that when the optical beam is deflected by the EIT medium, the wave packet will spread in the transverse direction. This spread will blur the observation of deflection. To examine this, we calculate the transverse fluctuation

$$\langle\Delta x^2\rangle = a^2\frac{1+\left(a^2b_1^2t^2-2\right)f_t\cos\alpha + \left(\cos^2\alpha - a^2b_1^2t^2\right)f_t^2}{(1-f_t\cos\alpha)^2}$$

with $b_0 = 0$. Usually, only if $\langle\Delta x^2\rangle < \langle x\rangle^2$, we can clearly observe such deflection. Otherwise, i.e., $\langle\Delta x^2\rangle > \langle x\rangle^2$, the deflection will be blurred by the transverse spreading of wave packets. In this case, a weak-measurement technique is necessary to observe the extremely small deflection of the light beam.

IV. WEAK VALUE AND DEFLECTION OF THE OPTICAL BEAM

In the previous section, we have shown that the projection measurement on the initial polarization described by the state $|i\rangle$ in Eq. (16) could induce transverse displacement of the optical beam after light passes through an EIT medium. Now, we will consider the maximization of this transverse displacement, with the weak measurement proposed by Aharanov *et al.* [1].

A weak measurement describes a situation where a system is so weakly coupled to a measuring device that the uncertainty in the measurement is larger than all the separations among the eigenvalues of the observable. Therefore, no information is given since the eigenvalues are not fully resolved. Three steps are necessary for weak measurements: (1) quantum state preparation (preselection); (2) a weak perturbation; (3) postselection on a final quantum state. The three essential ingredients of weak measurements were theoretically performed in the previous section.

First, we have initially prepared the state $|i\rangle$ of the system and a Gaussian wave packet of the meter before the light is incident on the medium. Second, the polarization-dependent effective potential in Eq. (14) changes the polarized state as

$$|\phi\rangle = \frac{e^{-i\bar{\theta}_x t}}{\sqrt{2}}\left[\exp\left(i\frac{\alpha+b_0 t}{2}\right)\exp\left(i\frac{b_1 x t}{2}\right)|\sigma_-\rangle + \exp\left(-i\frac{\alpha+b_0 t}{2}\right)\exp\left(-i\frac{b_1 x t}{2}\right)|\sigma_+\rangle\right] \tag{27}$$

with $\bar{\theta}_x = (\bar{b}_0 + \bar{b}_1 x)$, where $\bar{b}_j \equiv (b_{j+} + b_{j-})/2$. The state $|\phi\rangle$ indicates that there is an interaction Hamiltonian between the system and the meter, $H_{\rm int} = \xi\sigma_z$ with $\xi = b_1 x/2$, and a free evolution $\exp(-ib_0 t\sigma_z/2)$ for the spin. Here, $|\sigma_\pm\rangle$ are the eigenstates of the Pauli operator σ_z with eigenvalues ±1. A weak perturbation is guaranteed when the transverse displacement in momentum space is smaller than the width of the transverse distribution. In addition, the coupling strength b_1 can be adjusted by the control laser field and the magnetic field gradient.

Afterwards, the polarization state $|V\rangle$ is postselected. The information on the observable of the system is read out from the transverse spatial distribution which serves as the meter. However, the mean position in Eq. (26) is not the weak value. Weak measurements can provide the weak values defined by $\langle\sigma_z\rangle_w = \langle\psi_{\rm fi}|\hat{\sigma}_z|\psi_{\rm in}\rangle/\langle\psi_{\rm fi}|\psi_{\rm in}\rangle$, where $|\psi_{\rm in}\rangle$ and $|\psi_{\rm fi}\rangle$ are the preselected and postselected states of the system, respectively. Here, they are given by

$$|\psi_{\rm in}\rangle \equiv \frac{e^{-i\bar{\theta}_x t}}{\sqrt{2}}\left[\exp\left(i\frac{\alpha+b_0 t}{2}\right)|\sigma_-\rangle + \exp\left(-i\frac{\alpha+b_0 t}{2}\right)|\sigma_+\rangle\right], \tag{28a}$$

$$|\psi_{\rm fi}\rangle = |V\rangle. \tag{28b}$$

In our case, the observable is σ_z. Taking the free evolution of the spin into account, we obtain the weak value

$$\langle\sigma_z\rangle_w = \frac{\langle\psi_{\rm fi}|\sigma_z|\psi_{\rm in}\rangle}{\langle\psi_{\rm fi}|\psi_{\rm in}\rangle} = i\cot\left(\frac{\alpha+b_0 t}{2}\right). \tag{29}$$

From the definition of the weak value, one can find that if the free evolution of the spin is not taken into account, the resulting weak value is $i\cot(\alpha/2)$, rather than the above result.

It is well known that the weak value is linked to the final read of the meter. To obtain the mean position, one should first expand $\langle\psi_{\rm fi}|\exp(-i\xi\sigma_z t)|\psi_{\rm in}\rangle$ up to first order in $b_1 t$. Actually, this first-order expansion is valid in our system since we consider only the short-time behavior and the external magnetic field gradient B_1 in the x direction is very small; thus

$$b_1 t_f \ll a^{-1} \tag{30}$$

is satisfied, which is the condition for performing the weak measurement. Then we write $\langle\psi_{\rm fi}|\sigma_z|\psi_{\rm in}\rangle$ in terms of the weak value $\langle\sigma_z\rangle_w$. Finally, we regroup it to an exponential function $\langle\psi_{\rm fi}|\psi_{\rm in}\rangle(1 - i\xi t\langle\sigma_z\rangle_w) \approx \langle\psi_{\rm fi}|\psi_{\rm in}\rangle\exp(-i\xi t\langle\sigma_z\rangle_w)$, which yields

$$\langle x\rangle_{wv} = a^2 b_1 t\cot\left(\frac{\alpha+b_0 t}{2}\right) \tag{31}$$

as the observed mean position of the meter.

It can be seen from Eq. (31) that the final read of the meter is proportional to the imaginary part of the weak value. To find the relation between the result in Eq. (26) and the weak value in Eq. (31), we rewrite Eq. (18) as

$$|E_j(t)\rangle = \exp[-i(cp_z + b_{0j})t](1 - ib_{1j}xt)|E_0(0)\rangle \tag{32}$$

by retaining the linear term of the Taylor series expansion of $\exp(-ib_{1j}xt)$. After some algebra, we find that the mean position in Eq. (31) is a linear approximation of Eq. (26) with respect to the coupling between the system and the meter. After the postselection of the polarization degrees of freedom, the normalized wave packet of the probe field in the transverse direction becomes

$$\Psi_f^N(x,t) = \frac{1}{\sqrt{2\pi a^2}}\exp\left(-\frac{x^2 - x\langle x\rangle_{wv} + \langle x\rangle_{wv}^2}{4a^2}\right). \tag{33}$$

In Fig. 3, we plot the transverse distribution of the incident wave packet in Eq. (23) with a red solid curve, $|\Psi_f^N(x,t)|^2$ in Eq. (33) at time $t_f = L/c$ (black dashed curve), and the normalized norm squared of Eq. (19) right after the probe field leaves the atomic medium (green dash-dotted curve). Obviously, the weak measurement significantly enhances the deflection of the probe field.

Unlike the mean value of a quantum-mechanical measurement, which must lie within the range of eigenvalues, weak values in Eq. (29) produce results much larger than any of the eigenvalues of an observable, particularly when one chooses the initial state $|\psi_{\rm in}\rangle$ with $\alpha = -b_0 t_f$ (where t_f is the total interaction time). By performing a weak measurement of the probe laser field that has passed through an EIT atomic medium, we are able to significantly magnify the transverse displacement of the probe field, which results in a large group velocity $d\langle x\rangle_{wv}/dt$ in the transverse direction. The deflection

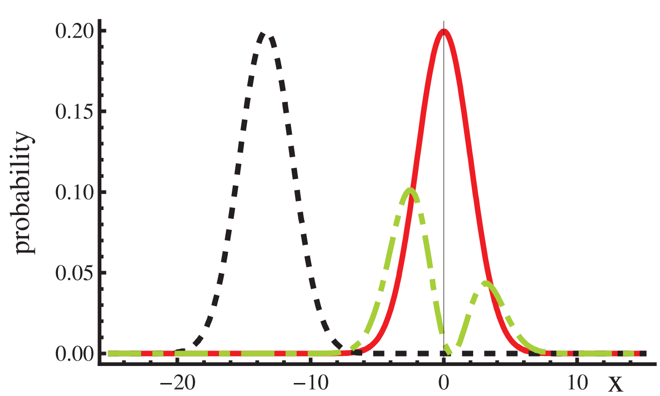

FIG. 3. (Color online) Transverse distribution of the probe field. The red solid curve corresponds to the Gaussian profile in Eq. (23). The black dashed curve depicts the norm squared of the wave function in Eq. (33) with a weak measurement right after the light leaves the medium. The green dash-dotted curve presents the normalized distribution of Eq. (19) at time $t_f = L/c$. Here, x is in units of millimeters. $b_0 t + \alpha = 0.08$. The other parameters are the same as in Fig. 2.

angle given in Ref. [21] is defined as $\theta = c^{-1} d\langle x\rangle_{wv}/dt$. When $b_0 = 0$, the deflection angle is totally decided by the original polarization angle α, and the magnitude of the deflection angle could be arbitrarily large as α approaches zero. Comparing to the angle of deflection 2×10^{-5} rad for the EIT condition [21], the weak-measurement technique discussed here greatly amplifies the displacement of the probe field in the transverse direction.

When the dynamics in the x direction is taken into account, the effective Hamiltonian in Eq. (21) becomes

$$H_j = cp_z + \frac{c}{2k}p_x^2 + b_{0j} + b_{1j}x.$$

After postselecting the system on a desired polarized state $|V\rangle$, the centroid of the wave packet shifts to

$$\langle x\rangle = \frac{ct^2}{k}\bar{b}_1 + \frac{e^{-f_{2t}}\sin(\alpha+f_{1t})\left(a^2t+\frac{c^2t^3}{2a^2k^2}\right)b_1}{1-\cos(\alpha+f_{1t})e^{-f_{2t}}},$$

where

$$f_{1t} = b_0t + \frac{ct^3}{3k}\bar{b}_1b_1, \quad f_{2t} = \left(\frac{c^2t^2}{8a^2k^2}+\frac{a^2}{2}\right)t^2b_1^2.$$

By expanding the above centroid of the wave packet up to first order in the coupling between the system and the meter, we obtain

$$\langle x\rangle = \frac{ct^2}{k}\bar{b}_1 + \left(a^2t+\frac{c^2t^3}{2a^2k^2}\right)b_1\cot\frac{\alpha+b_0t}{2}.$$

The terms related to $ct^2/(2k)$ and $c^2t^3/(2a^2k^2)$ yield the difference from the centroid of the wave packet in Eq. (31). We calculate the magnitude of each term at the time t_f by the data given in Sec. III, and found that $ct_f^2/(2k)\sim 10^{-19}$, $c^2t_f^3/(2a^2k^2)\sim 10^{-22}$, and $a^2t_f\sim 10^{-16}$, which shows that the term a^2t contributes most to the centroid of the wave packet. Therefore, we can neglect the transverse dynamics.

According to Ref. [25], there is a modification of the group velocity of the probe field in the EIT medium. In this case, Eq. (21) will be modified by replacing $c\rightarrow v_g = c\cos^2\theta$ and $|\Omega|^2\rightarrow|\Omega|^2+g^2N$, i.e., Eq. (21) becomes $H_j = v_gp_z + b'_{0j} + b'_{1j}x$, where b' is related to b by the expression $b'_{lj} = b_{lj}\cos^2\theta$ $(l=0,1)$. After some algebra, it can been found that the condition for allowing use of the weak-measurement technique and the weak value are still given by Eqs. (30) and (31), respectively. We note the difference between our semiclassical approach and the polariton approach. In our semiclassical approach, the atomic medium is treated as a quantum system and the probe field is treated as the classical system. The propagation velocity of the light remains unchanged, i.e., the speed of light c, but the "force" becomes large. In the polariton approach, both the probe light and the atomic medium are treated as quantum systems. The propagation velocity of the polariton is changed to $c\cos^2\theta$, but the force becomes small. However, the two approaches give the same results for light deflection.

V. DISCUSSION

We have theoretically studied a magneto-optically controlled atomic ensemble under the EIT condition to couple a property (the observable σ_z) of the polarization (the system) with the spatial degree of freedom (the meter). In the paraxial regime, the dynamics of the transverse distribution is governed by an impulsive measurement interaction Hamiltonian $H_{\text{int}} = \xi\sigma_z$, which makes the displacements of the transverse spatial components polarization dependent. An enhanced displacement in the meter distribution is achieved by an appropriate preselection and postselection of the polarization state. However, the choice of the preselected state is dependent on the accumulated phase during the free evolution of the system with the weak measurement taking place in between.

For an atomic gas in a finite temperature, the Doppler shift $k_{p,c}v$ for the atoms having velocity v along the probe or control-field propagation direction has to be involved in the detunings δ_j,δ_c. To neglect the Doppler-induced absorption, the EIT condition must be changed to $|\Omega|^2 \gg (\delta_j-\delta_c)k_{p,c}\bar{v},\gamma(\Gamma+k_{p,c}\bar{v})$, where $\bar{v}$ is the mean thermal atomic velocity and k_p and k_c are the wave numbers of the probe and control field. Integrating over the Maxwell-Boltzmann velocity distribution shows that b_{1j} in Eq. (21) remains unchanged; however, b_{0j} is related to the mean thermal atomic velocity. Consequently, the choice of the polarization angle α in Eq. (16) must be related to the mean atomic velocity in order to obtain the weak value.

Our previously study [20] shows that there is a polarization or quasispin current in this system, which is transverse to the flow of photons generated by the transverse gradient of magnetic fields. Weak measurements map the small polarization current onto a large shift of a measuring device's pointer. We notice that one can choose the magnetic moment of state $|s\rangle$ equal to that of one ground state (say $|-\rangle$); the σ_- component of the probe field propagates in a straight line, while the σ_+ component of the probe field experiences a declination similar to the probe field in Ref. [21], i.e., the tiny beam deflection is completely caused by the σ_+ component. Therefore, the weak-value technique significantly amplifies the beam deflection of the the probe field in Ref. [21].

Finally, we note that light can be stored in as many modes as possible in the collective excitations in an atomic ensemble with definite space variations. We hope that such a weak-value technique as discussed here can enhance the resolution for different modes stored in an atomic ensemble.

ACKNOWLEDGMENTS

This work is supported by NSFC Grants No. 11074071 and No. 11374095, NFRPC Grant No. 2012CB922103, Hunan Provincial Natural Science Foundation of China (Grants No. 11JJ7001 and No. 12JJ1002), the Scientific Research Fund of Hunan Provincial Education Department (Grant No. 11B076). F.N. is partially supported by the ARO, JSPS-RFBR Contract No. 12-02-92100, a Grant-in-Aid for Scientific Research (S), MEXT Kakenhi on Quantum Cybernetics, and the JSPS via its FIRST Program.

APPENDIX: EFFECTIVE EQUATION FOR THE PROBE FIELD WITH TRANSVERSE DYNAMICS

In this Appendix, we will derive the effective Schrödinger equation by taking the transverse dynamics into account. The effective Schrödinger equation is obtained by the following steps: First, we assume that the changes along the z direction of the probe envelope are smaller than the changes that occur along the transverse directions, which allows us to neglect the second-order derivative over the coordinates with respect to z and t for the amplitude $E_j(\mathbf{r},t)$ as well as the first-order derivative over time for atomic slowly varying variables Θ_{je}. We obtain the paraxial wave equation

$$i\partial_t E_j(r,t) + ic\partial_z E_j(r,t) + \frac{c}{2k}\nabla_T^2 E_j(r,t) = -g_j N\Theta_{je}. \tag{A1}$$

In the linear-optical-response theory, the paraxial wave equation further reduces to Eq. (10). For the atomic medium, we first obtain the Langevin equations for the atomic operators. In order to neglect the Langevin noise operators, we assume that the number of photons contained in the probe laser beams is much smaller than the number of atoms in the sample. Then the dynamics of the atomic ensemble is obtained as

$$\begin{aligned}\dot{\Theta}_{+e} &= (i\delta_+ - \Gamma)\Theta_{+e} + i\Omega\Theta_{+s} + ig_-E_-\Theta_{+-}\\ &\quad + ig_+E_+(\Theta_{++} - \Theta_{ee}), &\text{(A2a)}\\ \dot{\Theta}_{+s} &= [i(\delta_+ - \delta_c) - \gamma]\Theta_{+s} - ig_+E_+\Theta_{es} + i\Omega^*\Theta_{+e}, &\text{(A2b)}\\ \dot{\Theta}_{-e} &= (i\delta_- - \Gamma)\Theta_{-e} + i\Omega\Theta_{-s} + ig_+E_+\Theta_{-+}\\ &\quad + ig_-E_-(\Theta_{--} - \Theta_{ee}), &\text{(A2c)}\\ \dot{\Theta}_{-s} &= [i(\delta_- - \delta_c) - \gamma]\Theta_{-s} - ig_-E_-\Theta_{es} + i\Omega^*\Theta_{-e}, &\text{(A2d)}\end{aligned}$$

where we have phenomenologically introduced the relaxation rate Γ of the excited state and the decoherence rate γ. We note that the Doppler and collisional broadening are phenomenologically included in the coherence relaxation rate γ. Since we are interested in the situation that the intensity of the probe laser beams is much weaker than that of the control laser field, we use the perturbation approach, which is introduced in Eq. (6). The zeroth-order equations in g_jE_j read

$$\begin{aligned}\dot{\Theta}_{+e}^{[0]} &= (i\delta_+ - \Gamma)\Theta_{+e}^{[0]} + i\Omega\Theta_{+s}^{[0]}, &\text{(A3a)}\\ \dot{\Theta}_{+s}^{[0]} &= [i(\delta_+ - \delta_c) - \gamma]\Theta_{+s}^{[0]} + i\Omega^*\Theta_{+e}^{[0]}, &\text{(A3b)}\\ \dot{\Theta}_{-e}^{[0]} &= (i\delta_- - \Gamma)\Theta_{-e}^{[0]} + i\Omega\Theta_{-s}^{[0]}, &\text{(A3c)}\\ \dot{\Theta}_{-s}^{[0]} &= [i(\delta_- - \delta_c) - \gamma]\Theta_{-s}^{[0]} + i\Omega^*\Theta_{-e}^{[0]}, &\text{(A3d)}\end{aligned}$$

and the equations of first order in g_jE_j are

$$\begin{aligned}\dot{\Theta}_{+e}^{[1]} &= (i\delta_+ - \Gamma)\Theta_{+e}^{[1]} + i\Omega\Theta_{+s}^{[1]} + ig_-E_-\Theta_{+-}^{[0]}\\ &\quad + ig_+E_+\big(\Theta_{++}^{[0]} - \Theta_{ee}^{[0]}\big), &\text{(A4a)}\\ \dot{\Theta}_{+s}^{[1]} &= [i(\delta_+ - \delta_c) - \gamma]\Theta_{+s}^{[1]} - ig_+E_+\Theta_{es}^{[0]} + i\Omega^*\Theta_{+e}^{[1]}, &\text{(A4b)}\\ \dot{\Theta}_{-e}^{[1]} &= (i\delta_- - \Gamma)\Theta_{-e}^{[1]} + i\Omega\Theta_{-s}^{[1]} + ig_+E_+\Theta_{-+}^{[0]}\\ &\quad + ig_-E_-\big(\Theta_{--}^{[0]} - \Theta_{ee}^{[0]}\big), &\text{(A4c)}\\ \dot{\Theta}_{-s}^{[1]} &= [i(\delta_- - \delta_c) - \gamma]\Theta_{-s}^{[1]} - ig_-E_-\Theta_{es}^{[0]} + i\Omega^*\Theta_{-e}^{[1]}. &\text{(A4d)}\end{aligned}$$

We assume furthermore that the whole population of atoms is initially prepared in a mixed state of the ground states when the electromagnetic fields are absent. Since the population experiences no changes for the equations of the zeroth order in g_jE_j, only the terms $\Theta_{--}^{[0]}$ and $\Theta_{++}^{[0]}$ are different from zero, and $\Theta_{--}^{[0]} + \Theta_{++}^{[0]} = 1$. For a probe field with duration much larger than Γ^{-1} and γ^{-1}, the lowest adiabatic approximation allows us to let $\dot{\Theta}_{\alpha\beta}^{[1]} = 0$. The steady-state solutions give the relation between the atomic response $\Theta_{je}^{[1]}$ and the slow variable E_j of the probe field:

$$\Theta_{je}^{[1]} = \frac{g_j[(\delta_j - \delta_c) + i\gamma]\Theta_{jj}^{[0]}}{(i\delta_j - \Gamma)[i(\delta_j - \delta_c) - \gamma] + |\Omega|^2}E_j. \tag{A5}$$

The condition $|\Omega|^2 \gg \Gamma\gamma,\delta_i\delta_j$ reduces the above atomic response to

$$\Theta_{je}^{[1]} = \Theta_{jj}^{[0]}\frac{(\delta_j - \delta_c) + i\gamma}{|\Omega|^2}g_jE_j, \tag{A6}$$

which reduces to Eq. (8) by letting $\gamma = 0$ and $\Theta_{jj}^{[0]} = 1/2$. Substituting $\Theta_{je}^{[1]}$ into Eq. (A1), we obtain the equation for the spatial motion of the probe field:

$$\begin{aligned}&i\partial_t E_j(r,t) + ic\partial_z E_j(r,t) + \frac{c}{2k}\nabla_T^2 E_j(r,t)\\ &\quad = -\Theta_{jj}^{[0]}\frac{(\delta_j - \delta_c) + i\gamma}{|\Omega|^2}|g_j|^2NE_j. \end{aligned}\tag{A7}$$

Therefore, the propagation velocity of the light along the z direction is the speed of light. We note that the decoherence rate $\gamma \approx 10^{-4}\Gamma$ leads to absorption of the probe field by the atomic ensemble, where the relaxation rate Γ is of the order of megahertz. From the data presented in Sec. III, the ratio of the output intensity of the probe field to its input intensity is approximately $\exp(-10^{-3})$, and the magnitude of detuning $\delta_+ - \delta_c$ is about $10^{-2}\Gamma$, which means that the detuning $\delta_j - \delta_c$ plays the major role. In order to show the underlying physics, we let $\gamma = 0$. In the following, our treatment proceeds in only one transverse dimension, say in the x direction. By defining $p_z = -i\partial_z$ and $p_x = -i\partial_x$, the paraxial wave equation becomes a Schrödinger-like equation. So we can define the effective Hamiltonian

$$H = cp_z + \frac{c}{2k}p_x^2 - \frac{N|g_j|^2}{|\Omega|^2}\Theta_{jj}^{[0]}(\delta_j - \delta_c). \tag{A8}$$

Equation (12) is obtained by neglecting the transverse momentum. It can been found that an initial mixed state with an imbalance of the populations changes the value of b_{0j} and b_{1j} in Eq. (21) by replacing $1/2 \to \Theta_{jj}^{[0]}$ in Eq. (22). Hence, the observed mean position of the meter in Eq. (31) is changed accordingly, and so is the choice of the polarization angle α in Eq. (16) to enlarge the observed mean position of the meter in Eq. (31).

[1] Y. Aharonov, D. Z. Albert, and L. Vaidman, Phys. Rev. Lett. **60**, 1351 (1988).
[2] Y. Aharonov and D. Rohrlich, *Quantum Paradoxes—Quantum Theory for the Perplexed* (WILEY-VCH, Weinheim, 2005).
[3] J. V Neumann, *Mathematical Foundations of Quantum Mechanics* (Princeton University Press, Princeton, NJ, 1955); published in German 1932.
[4] A. G. Kofman, S. Ashhab, and F. Nori, Phys. Rep. **520**, 43 (2012).
[5] N. W. M. Ritchie, J. G. Story, and R. G. Hulet, Phys. Rev. Lett. **66**, 1107 (1991).
[6] G. J. Pryde, J. L. O'Brien, A. G. White, T. C. Ralph, and H. M. Wiseman, Phys. Rev. Lett. **94**, 220405 (2005).
[7] P. B. Dixon, D. J. Starling, A. N. Jordan, and J. C. Howell, Phys. Rev. Lett. **102**, 173601 (2009).
[8] Q. Wang, F.-W. Sun, Y.-S. Zhang, Jian-Li, Y.-F. Huang, and G.-C. Guo, Phys. Rev. A **73**, 023814 (2006).
[9] N. S. Williams and A. N. Jordan, Phys. Rev. Lett. **100**, 026804 (2008).
[10] A. Romito, Y. Gefen, and Y. M. Blanter, Phys. Rev. Lett. **100**, 056801 (2008).
[11] N. Brunner, V. Scarani, M. Wegmüller, M. Legré, and N. Gisin, Phys. Rev. Lett. **93**, 203902 (2004).
[12] K. Y. Bliokh and Y. P. Bliokh, Phys. Rev. Lett. **96**, 073903 (2006).
[13] O. Hosten and P. Kwiat, Science **319**, 787 (2008).
[14] F. Nori, Nat. Photonics **2**, 717 (2008).
[15] K. Y. Bliokh, A. Niv, V. Kleiner, and E. Hasman, Nat. Photonics **2**, 748 (2008).
[16] Y. Gorodetski, K. Y. Bliokh, B. Stein, C. Genet, N. Shitrit, V. Kleiner, E. Hasman, and T. W. Ebbesen, Phys. Rev. Lett. **109**, 013901 (2012).
[17] D. L. Zhou, L. Zhou, R. Q. Wang, S. Yi, and C. P. Sun, Phys. Rev. A **76**, 055801 (2007).
[18] L. Zhou, J. Lu, D. L. Zhou, and C. P. Sun, Phys. Rev. A **77**, 023816 (2008).
[19] H. R. Zhang, L. Zhou, and C. P. Sun, Phys. Rev. A **80**, 013812 (2009).
[20] Y. Guo, L. Zhou, L. M. Kuang, and C. P. Sun, Phys. Rev. A **78**, 013833 (2008).
[21] L. Karpa and M. Weitz, Nat. Phys. **2**, 332 (2006).
[22] E. Knill, R. Laflamme, and G. J. Milburn, Nature (London) **409**, 46 (2001).
[23] Z. Y. Ou and L. Mandel, Phys. Rev. Lett. **61**, 50 (1988).
[24] M. Fleischhauer and M. D. Lukin, Phys. Rev. Lett. **84**, 5094 (2000).
[25] M. Fleischhauer and M. D. Lukin, Phys. Rev. A **65**, 022314 (2002).
[26] C. P. Sun, Y. Li, and X. F. Liu, Phys. Rev. Lett. **91**, 147903 (2003).
[27] D. Petrosyan and Y. P. Malakyan, Phys. Rev. A **70**, 023822 (2004).
[28] Y. Aharonov and L. Vaidman, Phys. Rev. A **41**, 11 (1990).
[29] L. Karpa, F. Vewinger, and M. Weitz, Phys. Rev. Lett. **101**, 170406 (2008).